2018

Behavior of Steel Furnace Slag, Coal Wash, and Rubber Crumb Mixtures with Special Relevance to Stress-Dilatancy Relation

Yujie Qi
University of Wollongong, qyujie@uow.edu.au

Buddhima Indraratna
University of Wollongong, indra@uow.edu.au

J S. Vinod
University of Wollongong, vinod@uow.edu.au

Behavior of Steel Furnace Slag, Coal Wash, and Rubber Crumb Mixtures with Special Relevance to Stress-Dilatancy Relation

Abstract

The influence of rubber crumbs on the dilatancy behavior and critical state of steel furnace slag (SFS), coal wash (CW), and rubber crumbs (RC) mixtures was investigated via a series of monotonic drained triaxial tests. These tests revealed that RC contents (R_b, %) have a significant influence on the dilatancy behavior and critical state of the aforementioned waste mixtures; in fact, as more R_b is added, dilatancy and the slope of the critical state line in e–ln p' space decreases. Within the framework of critical state soil mechanics, a dilatancy model for SFS+CW+RC mixtures was proposed and validated using experimental data. This model also captured the energy-absorbing property of RC using an empirical relationship between the total work input W_{total} and the critical stress ratio M_{cs}.

Disciplines

Engineering | Science and Technology Studies

Publication Details

Qi, Y., Indraratna, B. & Vinod, J. S. (2018). Behavior of Steel Furnace Slag, Coal Wash, and Rubber Crumb Mixtures with Special Relevance to Stress-Dilatancy Relation. Journal Of Materials In Civil Engineering, 30 (11), 04018276-1-04018276-10.

Behavior of Steel Furnace Slag, Coal Wash, and Rubber Crumb Mixtures, with Special Relevance to Stress-dilatancy Relation

Yujie Qi

PhD, Ms, Bs
Research Associate, Centre for Geomechanics and Railway Engineering, ARC Industry Transformation Training Centre for Advanced Rail Track Technologies, Faculty of Engineering, University of Wollongong, Wollongong, NSW 2522, Australia

Buddhima Indraratna

PhD (Alberta), MSc and BSc-Hons (London), FTSE, FIEAust, FASCE, FGS, FAusIMM, FIES, DIC, CEng, CPEng
Distinguished Professor, Research Director and Foundation Director, Civil Engineering, Centre for Geomechanics and Railway Engineering, ARC Industry Transformation Training Centre for Advanced Rail Track Technologies, Faculty of Engineering, University of Wollongong, Wollongong, NSW 2522, Australia

Jayan S. Vinod

PhD, M.Tech. B.Tech.
Associate Professor, Centre for Geomechanics and Railway Engineering, ARC Industry Transformation Training Centre for Advanced Rail Track Technologies, Faculty of Engineering and Information Sciences, University of Wollongong, Wollongong, NSW 2522, Australia

†Author for correspondence:
Dr Jayan S. Vinod
School of Civil, Mining, and Environmental Engineering,
Faculty of Engineering and Information Sciences, University of Wollongong
Wollongong, NSW 2522
AUSTRALIA
Ph: +61 02 4221 4089
Email: vinod@uow.edu.au

Published by: Journal of Materials in Civil Engineering

Abstract: The influence of rubber crumbs on the dilatancy behavior and critical state of SFS+CW+RC mixtures (i.e., blends of steel furnace slag, coal wash, and rubber crumbs) has been investigated via a series of monotonic drained triaxial tests. These tests reveal that RC contents (R_b, %) have a significant influence on the dilatancy behavior and critical state of the aforementioned waste mixtures; in fact as more R_b is added, dilatancy and the slope of the critical state line in $e - \ln p'$ space decreases. Within the framework of critical state soil mechanics, a dilatancy model for SFS+CW+RC mixtures has been proposed and validated using experimental data. This model also captured the energy absorbing property of RC using an empirical relationship between the total work input W_{total} and the critical stress ratio M_{cs}.

KEYWORDS: Steel furnace slag; coal wash; rubber crumbs; critical state; energy absorbing property; dilatancy

Introduction

Steel furnace slag (SFS) and coal wash (CW) are waste by-products of steel making and coal mining, whereas rubber crumbs (RC) are derived from waste tires, and since they occupy large amounts of useable land their long term effect on the environment is extremely detrimental. One of the best ways of dealing with these materials is to recycle them into geotechnical projects such as port reclamations, where different blends of SFS+CW have already been used successfully (Chiaro et al., 2013). However, while incorporating RC into SFS+CW blends can further reduce the particle breakage of CW and swelling of SFS, as well as increasing the energy absorbing capacity of these waste mixtures, a better understanding of the effect that RC has on the geotechnical behavior of SFS+CW+RC mixtures from a mathematical perspective is urgently needed. Despite the research already carried out to investigate the behavior of soil-rubber mixtures in the laboratory, only a few focused on the theoretical models used to predict the behavior of soil-rubber mixtures.

Stress-dilatancy is a fundamental aspect needed to model the stress-strain behavior of soil. It has been suggested that dilatancy in its initial form is a unique function with the stress ratio η (Taylor, 1948), but granular materials differ from cohesive soils, so dilatancy not only depends on η but also on the density and stress history of soil (e.g. Rowe, 1962; Nova and Wood, 1979). To avoid using too many parameters for a single granular material with different initial conditions, Been and Jefferies (1985) introduced a state parameter ψ based on a critical state concept which relates the density and stress history of soil. Until now ψ and the critical state concept has been widely used to model the dilatancy of granular materials (e.g. Wan and Guo, 1998; Li and Dafalias, 2000; Wang et al., 1990); more recently they have also been successfully extended to tire chips/shreds – sand mixtures (e.g. Mashiri et al., 2015; Youwai and Bergado, 2003).

However, only limited studies have been carried out on the dilatancy behavior of tire soil mixtures (e.g. Mashiri et al. 2015). Mashiri et al. (2015) has developed a dilatancy model for sand-tire chip mixtures. It is to be noted that currently there is no or very limited literature available on the dilatancy behavior of waste mixture –tire crumb mixtures. Rubber crumbs behave differently with tire chips. Tire chips are relatively larger pieces of tire derived aggregate (typically the size of a gravel) that may also include reinforcing elements such as polymeric fibres (of various types) and/or steel fibres from remaining wire reinforcement (Mashiri et al., 2017; Fu et al., 2017). Thus, tire chips look and behave more like a composite material whereas rubber crumbs is made of (and behave more like) a single material (i.e., just rubber). As a result, these two are inherently different materials with corresponding mechanical behavior reflecting their original constituents (i.e., rubber crumbs is mainly isotropic whereas tire chips may behave anisotropically due to the presence of any reinforcing inclusions still present in the chips) (Mashiri et al., 2017). Therefore, previous investigations on tire chips/shreds-soil mixtures cannot totally reflect the behavior of RC-waste mixtures.

Moreover, no previous studies have incorporated the energy absorbing property of RC in modelling rubber-soil materials. As energy absorbing capacity is a very important geotechnical property of rubber materials, it is important to incorporate its influence when modelling the behavior of RC-waste mixtures. Therefore, in this study the dilatancy behavior of SFS+CW+RC mixtures was investigated based on a series of monotonic drained triaxial tests. The critical state and the energy absorbing property of the mixtures were also examined.

Materials and Methodology

The coal wash (specific gravity $G_s = 2.11$) and steel furnace slag ($G_s = 3.43$) used in this study are from Illawarra Coal and Australia Steel Milling Services, respectively. The

96 granulated RC ($G_s = 1.15$) from waste tires are in three different size (0-2.3 mm, 0.3-3 mm,
97 and 1-7 mm); the appearance of these waste materials can be seen in Fig.1, and the particle
98 size distribution (PSD) curves of SFS, CW, and RC are shown in Fig.2. Form Fig.1, it can be
99 seen that the CW aggregates are composed of both angular and relatively flaky grains, RC are
100 dark angular granulated particles, while SFS is grey and tends to be a bit round. Based on the
101 unified soil classification system, SFS and CW are classified as well-graded gravel with silty-
102 sand, and well-graded sand with gravel, respectively.

103 As gradation can influence the behavior of soils (Salvatore et al., 2015), all the mixtures
104 tested in this study are mixed to the same gradation (the target PSD) shown in Fig.2. The
105 blending ratio of SFS and CW is 7:3 (by weight) because with this ratio the SFS+CW blends
106 have a relatively low particle breakage and swelling potential while maintaining a high shear
107 strength (Indraratna et al., 2017). The RC contents are 0%, 10%, 20%, 30%, 40% by weight;
108 every specimen was prepared with the optimum moisture content and then compacted to
109 achieve an initial dry unit weight equal to 95% of their maximum dry density. To achieve the
110 target particle size distribution (PSD), the preparation method followed a previous study by
111 Tasalloti et al. (2015). The waste materials were sieved and separated into different particle
112 sizes. For each SFS+CW+RC mixture, the dry mass required of each particle size was back-
113 calculated based on the target PSD curve, and then the exact mass corresponding to a given
114 size range was weighed and mixed thoroughly to obtain a uniform blend.

115 After the dried mixtures were prepared, the required amount of water was added to the
116 mixture, and the mixture was blended thoroughly. The triaxial test specimen (50mm in
117 diameter and 100 mm high) was then prepared and compacted using a split mould. Each
118 specimen was compacted in 5 layers using a drop hammer. Before placing the subsequent
119 layer, the previous layer was roughened to avoid any layering during the shearing.

120 The monotonic triaxial tests were carried out in accordance with ASTM D7181 (2011) and in
121 three stages, i.e. saturation, consolidation, and shearing. During saturation stage, the air was
122 firstly expelled by flooding the specimen(s) from the bottom with de-aired water, and then
123 the specimen was saturated with back pressure until the Skempton's B-value > 0.98. Isotropic
124 consolidation was then applied with an effective confining pressure of σ'_3 (10, 40 or 70 kPa).
125 After consolidation, the specimen was sheared under drained conditions at a constant strain
126 rate of 0.2 mm/min until 25% axial strain was reached. For each RC content, at the same test
127 conditions, at least two replicated tests have been done. For instance, a replicated test for
128 SFS+CW+RC mixtures with 40% RC has been shown in Fig.3 (c) and (f). It is evident that
129 the replicated test closely predicts the same (original test) behavior of SFS+CW+RC mixtures
130 with 40% RC at $\sigma'_3 = 70\ kPa$. The test number, dry density of each sample, as well as the
131 initial void ratio after consolidation (before shearing) are shown in Table 1.

132 **Experimental Results and Analysis**

133 ***Stress-strain behavior***

134 Fig.3 shows the typical stress-strain curves for SFS+CW+RC mixtures with different R_b (%)
135 at different confining pressures, i.e. $\sigma'_3 = 10, 40, \text{and } 70\ kPa$. From Fig.3(a-c) it can be
136 observed that the peak deviator stress q_{peak} increases as σ'_3 increases, but it decreases as R_b
137 (%) increases indicating the low shear strength of rubber crumbs. As more RC is included,
138 the axial strain corresponding to q_{peak} increases as the specimen changes from brittle to
139 ductile. This may be attributed to the increase of rubber-to-rubber interaction in
140 SFS+CW+RC mixtures (Sheikh et al., 2013). Moreover, all the specimens exhibited a
141 predominantly strain softening behavior accompanied by a contractive-dilative response.

142 The inclusion of RC also affects the strain behavior of SFS+CW+RC mixtures (Fig.3 d-f). As
143 expected, the waste mixtures become much more contractive as R_b (%) increases because of

the high compressibility of rubber materials. Under the effective confining pressure $\sigma'_3 = 10, 40, \text{and } 70\ kPa$, the volumetric strain of specimens with $R_b \leq 10\%$ all reached a stable state before the end of the test, whereas those with $R_b \geq 20\%$ still keep dilation by the end of the test.

Dilatancy behavior

Dilatancy is one of the fundamental components in modelling the stress-strain behavior of a soil. It is the ratio of the increment of plastic volumetric strain to the increment of plastic deviator strain in triaxial space (Nova and Wood, 1979; Wood and Belkheir, 1994):

$$d = \frac{d\varepsilon_v^p}{d\varepsilon_q^p} \tag{1}$$

where $d\varepsilon_v = d\varepsilon_1 + 2d\varepsilon_3$, $d\varepsilon_q = 2(d\varepsilon_1 - d\varepsilon_3)/3$, and the superscript '$p$' stands for 'plastic'. The best way to investigate the dilatancy of soils is to plot dilatancy with a variation of the stress ratio η

$$\eta = q/p' \tag{2}$$

where $q = \sigma'_1 - \sigma'_3$ is the deviator stress in a triaxial setting, and $p' = (\sigma'_1 + 2\sigma'_3)/3$ is the effective mean stress.

Fig.4 (a-e) present the stress ratio-dilatancy curves at different effective confining pressures for SFS+CW+RC mixtures. Note there are three stress ratios of interest for the stress ratio-dilatancy curves, i.e. η_{PTS}, η_{peak}, and η_{CS} where PTS stands for the phase transformation state, 'peak' refers to the peak deviator stress state, and CS means the critical state. Thus the stress ratio at these three conditions $\eta_{PTS,peak,CS}$ can be determined by:

$$\eta_{PTS,peak,CS} = \frac{q_{PTS,peak,CS}}{p'_{PTS,peak,CS}} \tag{3}$$

Where $q_{PTS,peak,CS}$ is the deviator stress at the phase transformation state, the peak deviator stress state, or the critical state; and $p'_{PTS,peak,CS}$ is the effective mean stress at the phase transformation state, the peak deviator stress state, or the critical state. Moreover, η_{CS} can also be written as M_{cs}.

At the phase transformation state $d = 0$, the volumetric strain ε_v reaches its minimum value and the specimen changes from contraction to dilatancy. At the peak deviator stress state, the stress ratio η and the deviator stress reach their peak, and at the critical state $\eta_{CS} = M_{cs}$, $d = 0$, and $d\eta = 0$. Note that η_{peak} and η_{PTS} decrease as the effective confining pressure increases, and all the SFS+CW+RC specimens experience a hook after the peak deviator stress state. It is observed that only the dilatancy of SFS+CW+RC mixtures with 0% and 10% RC can reach zero after the peak deviator stress state (Fig.4 a & b), but as more RC are included $d = 0$ is harder to reach, whereas the trend of dilatancy indicates it is still possible to achieve zero beyond the 25% of axial strain.

Fig.4 (f & g) show the stress ratio-dilatancy curves of the waste mixtures with different R_b (%), which proves that R_b has a significant influence on the dilatancy of waste mixtures. At the same effective confining pressure, the peak stress ratio η_{peak} decreases as the R_b increases due to the low shear strength. As expected, dilatancy at η_{peak} decreases with the inclusion of RC because rubber materials are highly compressible, however the initial slope of the dilatancy curve is similar regardless of amount of RC.

The critical state of SFS+CW+RC mixtures

The critical state (CS) of conventional soils is when it reaches a condition where $\frac{dq}{d\varepsilon_q} = \frac{dp}{d\varepsilon_q} = \frac{d\varepsilon_v}{d\varepsilon_q} = 0$; this means that once CS arrives, there will be no further changes in the deviator stress and mean effective stress upon further straining the soil, and dilatancy also reaches

185 zero. To investigate the critical state of SFS+CW+RC mixtures, triaxial tests were carried out
186 to the maximum axial strain possible in the apparatus; it was generally around 25%.

187 Fu et al. (2017) investigated the effect of rubber particle type on the critical state of sand-
188 rubber mixtures, and the test results showed that with low rubber content (10%) granulated
189 rubber-sand mixtures can reach critical state within 25% of ε_1, while rubber buffing fibres-
190 sand mixtures can only reach critical state at very large axial strain (i.e. >40%). Mashiri et al.
191 (2015) found that mixtures of tire chips-sand with large amounts of rubber chips cannot reach
192 CS, even when $\varepsilon_1 = 25\%$, because tire chips keep on deforming until the end of the test
193 (Youwai and Bergado, 2003). However, RC is much smaller than tire chips, and when they
194 are compressed they will be surrounded by rigid particles (i.e. SFS and CW) which may
195 prevent further deformation of RC particles. In this study, the SFS+CW+RC mixtures with
196 lower R_b (0% and 10%) can directly achieve CS, whereas those with higher R_b (20-40%)
197 cannot reach CS by the test, albeit it is still possible to reach CS beyond $\varepsilon_1 = 25\%$ (e.g. Fig.4
198 c-e). Therefore, based on R_b (%), two ways for determining the CS for SFS+CW+RC
199 mixtures are suggested:

200 (1) With lesser R_b (0% and 10%), the CS of the SFS+CW+RC mixtures can be obtained
201 by comparing the curves in the$\varepsilon_q - \eta$, $\varepsilon_q - \varepsilon_v$, and $d - \eta$ spaces. An example of an
202 SFS+CW+RC mixture with 10% RC at $\sigma'_3 = 10\ kPa$ is shown in Fig.5 (a & b); here
203 dilatancy decreases after η_{peak} and reaches zero when the stress ratio $\eta = 2.01$
204 (Fig.5b). Meanwhile, the increment of $\frac{q}{p'} - \varepsilon_q$ and $\varepsilon_v - \varepsilon_q$ curves also reaches zero at
205 the same point (Fig.5a), so the critical state of the SFS+CW+RC mixture with 10%
206 RC is now determined ($M_{cs} = 2.01$).
207 (2) The CS of mixtures with larger R_b (20%, 30% and 40%), can be determined by
208 extrapolating the curves to the most probable value; Carrera et al. (2011), Indraratna

et al. (2014), and Modoni et al. (2011) also used this method. Fig.5 (c & d) show an example of an SFS+CW+RC mixture with R_b =30% at $\sigma'_3 = 40\ kPa$. Here the critical stress ratio is predicted from the stress ratio-dilatancy curve by extending the last part of the curve to the point of intersection with the zero dilatancy axes (Fig.5d). The $\eta - \varepsilon_q$ curve and $\varepsilon_v - \varepsilon_q$ curve are also extrapolated until the constant η and ε_v are obtained, and thus $M_{cs} = 1.61$ has been determined.

The value of M_{cs} and the critical void ratio e_{cs} of the waste mixtures are shown in Table 1. The results reveal that M_{cs} is no longer a constant for SFS+CW+RC mixtures since it depends on the effective confining pressure and R_b (%). In the $e_{cs} - \ln p'_{cs}$ space a linear relationship was established for the critical state line of the SFS+CW+RC mixtures (Fig.6a):

$$e_{cs} = \Gamma - \lambda \ln p'_{cs} \tag{4}$$

where Γ is the void ratio at $p'_{cs} = 1\ kPa$, and λ is the gradient of the critical state line in $e - \ln p'$ space. It is worthy to note that the critical state lines in $e - \ln p'$ space rotate clockwise as R_b (%) increases, thus indicating that Γ and λ are parameters associated with R_b (%) (Fig.6a). As expected, Fig.6 (b) shows that Γ and λ are in a linear relationship with R_b (%):

$$\Gamma^* = \Gamma_1 + \Gamma_2 R_b \tag{5}$$

$$\lambda^* = \lambda_1 + \lambda_2 R_b \tag{6}$$

where Γ^* and λ^* are the critical state parameters modified R_b. Γ_1, Γ_2, λ_1, and λ_2 are the calibration parameters calculated by the test data of Group A (waste mixtures with 0%, 10%, and 30% RC), and test data form Group B (waste mixtures with 20% and 40% RC) that were set separately and used for validation. There is a good agreement between the proposed empirical equations and the test data from Group B (Fig.6b).

Energy absorbing property of SFS+CW+RC mixtures

The energy absorbing property of SFS+CW+RC mixtures is captured by examining the total work W_{total} until the specimen achieved its point of failure. Here failure is taken to correspond to the peak deviator stress attained, which is in the same way as Zornberg et al. (2004) for Sand-tire shred mixtures. In general, the work given to a unit volume of SFS+CW+RC mixtures upon the applied stresses is partly consumed by friction due to particles rearrangement, and partly used by particles deformation. As the deformation of the rigid particles (i.e. SFS and CW) is negligible, the energy consumed by particle deformation is only occurred to RC. This also explains why rubber materials have high energy absorbing capacity (Zheng and Sutter, 2000). Two components are distinguished in the total work, i.e. volumetric and deviatoric, and by decoupling these two components, the increment of W applied onto the sample can be determined (Modoni et al., 2011)

$$dW_{total} = p'd\varepsilon_v + qd\varepsilon_q \tag{7}$$

The value of W_{total} of the mixtures is shown in Table 1. It is worthy to note that W_{total} is a parameter that incorporates the effects of R_b and the applied stress, and it increases as R_b and the confining stress increases. As mentioned above, M_{cs} is not a constant as it changes with confining stress and R_b. Therefore, W_{total} may be a good parameter to reflect the changes of M_{cs}. Chavez and Alonso (2003) proposed a model for rockfill using the plastic work to capture the changes of M_{cs} due to suction and confining stress. However, in this study as the elastic deformation generated by RC cannot be neglected, and thus the total work W_{total} is used to reflect the changes of M_{cs} due to confining stress and R_b. By connecting W_{total} to M_{cs}, an empirical relationship is established using group A data (Fig.7). In this way, the energy absorbing property of RC is translated through W_{total}. The equation is then validated by using group B data (independent set of data):

$$M_{cs}^{*} = M_0 * (\frac{W_{total}}{W_0})^{\alpha} \quad (8)$$

where M_0 is the critical stress ratio when $W_{total} = 1\ kPa$, α is a regression coefficient, and $W_0 = 1\ kPa$ is used to keep the unit of both side of the equation the same. It is evident that Equation (8) has a good correlation with independent set of data (Group B).

Dilatancy Model and Simulation for SFS+CW+RC Mixtures

The dilatancy of soil is usually related to the state of soil which corresponds to its density and pressures. Been and Jefferies (1985) proposed a state parameter ψ to capture the influence of the density and stress on the deformation of soils, where this state parameter is defined as the difference between the current void ratio and the critical void ratio at the same pressure:

$$\psi = e - e_{cs} \quad (9)$$

Fig.8 shows the definition of the state parameter. All the specimens of waste mixtures tested in this study were in a dense state after consolidation, so only $\psi < 0$ appeared. After consolidation at the same effective confining pressure, the initial void ratio of the SFS+CW+RC mixtures with a greater R_b (%) is smaller than those with less R_b (%), thus proving the high compressibility of rubber materials. As mentioned previously, the critical void ratio of the waste mixtures is related to R_b (%), therefore the state parameter ψ can be modified as:

$$\psi^{*} = e - (\Gamma^{*} - \lambda^{*} \ln p'_{CS}) \quad (10)$$

Following, Li and Dafalias (2000), the dilatancy of soil d associated with the state parameter, and is expressed as:

$$d = \frac{d\varepsilon_v^p}{d\varepsilon_q^p} = d_0 \left(e^{m\psi^{*}} - \frac{\eta}{M_{cs}^{*}} \right) \quad (11)$$

where d_0 and m are two material parameters, M_{cs}^* is the critical stress ratio modified with W_{total}, and ψ^* is the state parameter modified with R_b (%).

Parameter m can be computed based on the phase transformation state (PTS), i.e., $d = 0$, $\psi^* = \psi_{PTS}^*$, and $\eta = \eta_{PTS}$. Hence,

$$m = \frac{1}{\psi_{PTS}^*} \ln\left(\frac{\eta_{PTS}}{M_{cs}^*}\right) \tag{12}$$

The dilatancy parameter d_0 can be calculated at the peak deviator point, i.e., $d = d_{peak}$, $\psi^* = \psi^*{}_{peak}$, and $\eta = \eta_{peak}$. Thus,

$$d_0 = \frac{d_{peak}}{\left(e^{m\psi^*{}_{peak}} - \frac{\eta_{peak}}{M_{cs}^*}\right)} \tag{13}$$

The value of the dilatancy parameters is listed in Table 2. The parameters from Group A were calculated from the tests data, and parameters for group B were calculated based on Equations (8 and 10). Fig.9 (a-c) illustrate the dilatancy model predictions for SFS+CW+RC mixtures with 10%, 30%, and 40% RC at different effective confining pressures. Fig.9 (d) shows a comparison of the dilatancy model predictions with test results of mixtures with different R_b (%) at $\sigma'_3 = 70\ kPa$. Note that the dilatancy model clearly captures the dilatancy of SFS+CW+RC mixtures using the parameters from Group A and Group B, thus verifying the dilatancy model for the SFS+CW+RC mixtures.

Conclusions

This paper has investigated the stress-strain behavior (with special relevance to dilatancy and the critical state) of SFS+CW+RC mixtures with SFS:CW=7:3 and different RC contents R_b (%) through monotonic triaxial tests. It has been found that R_b (%) significantly influences the stress-strain behavior and the critical behavior of waste mixtures such that their shear strength and dilatancy decrease as R_b (%) increases mainly due to the low strength and

compressible nature of the rubber. Moreover, when $R_b < 20\%$, the CS of the waste mixtures can be achieved directly but when $R_b \geq 20\%$, the CS could not be achieved by the test, albeit the trend of $\eta - d$ curve showed that CS might be achieved beyond $\varepsilon_1 = 25\%$; thus extrapolation was used for waste mixtures with $R_b \geq 20\%$. On the $e - \ln p'$ plane, a linear relationship was proposed for the critical state line dependent on R_b (%). Moreover, the changing M_{cs} due to R_b and confining stress was reflected by the parameter W_{total} through an empirical function, and this equation also provides a way relating the energy absorbing property with M_{cs}.

The dilatancy behavior of the SFS+CW+RC mixture was predicted by a modified dilatancy function. In this function the energy absorbing property of RC was captured through the relationship of M_{cs}^* and W_{total}, while the dilatancy behavior with the variation of R_b (%) was also translated by the modified state parameter ψ^*. This dilatancy model agrees very well with the experimental data. Although this dilatancy function was developed for the SFS+CW+RC mixture, the method used to capture the energy absorbing property of rubber materials and the way of determining the critical state parameters can be a good reference for other mixtures of rubber and soil.

Notions

CS = critical state, and the critical state line, respectively;

CW = coal wash;

d = dilatancy

d_0 = dilatancy parameter;

d_{peak} = dilatancy at peak deviator stress state;

$d\varepsilon_v, d\varepsilon_v^p$ = total and plastic volumetric strain increment, respectively;

$d\varepsilon_q, d{\varepsilon_q}^p$ = total and plastic deviator strain increment, respectively;

dW_{total} = the increment of total work input;

e, e_0, e_{cs} = void ratio, the initial void ratio after consolidation, and the void ratio at critical state, respectively;

G_s = specific gravity;

m = dilatancy parameter;

M_0 = is the critical stress ratio when $W_{total} = 1\ kPa$;

M_{cs}, M_{cs}^* = the critical state stress ratio and the modified critical state ratio;

PTS = phase transformation state;

PSD = particle size distribution;

p', p'_{cs} = the effective mean stress and the effective mean stress at critical state (kPa), respectively;

q = the deviator stress (kPa);

R_b = the RC content (%);

RC = rubber crumbs;

SFS = steel furnace slag;

W_{total} = the total work input up to failure (kPa);

α = materials constant related to the total work input W_{total} and critical stress ratio M_{cs};

σ'_3 = the effective confining pressure (kPa) ;

ε_v, ε_q = the volumetric and deviator strain;

η = the stress ratio;

$\eta_{PTS}, \eta_{peak}, \eta_{CS}$ = the stress ratio at phase transformation state, peak deviator stress state, and critical state respectively;

Γ, Γ^* = void ratio at $p'_{cs} = 1\ kPa$ and modified Γ, respectively;

Γ_1, Γ_2 = calibration parameters for Γ;

λ, λ^* = the gradient of the critical state line in $e - \ln p'$ space, and modified λ, respectively;

λ_1, λ_2 = calibration parameters for λ;

ψ, ψ^* = state parameter and modified state parameter, respectively;

$\psi^*_{peak}, \psi^*_{PTS}$ = modified state parameter at peak deviator stress state and phase transformation state, respectively;

Acknowledgements

The first author would like to acknowledge the financial assistance provided by the China Scholarship Council. The assistance provided by industry (ASMS and South 32) in relation to the procurement of material used in this study is gratefully acknowledged. Assistance in the laboratory from Mr. Richard Berndt and occasional technical feedback from A/Prof Cholachat Rujikiatkamjorn and Dr Ana Heitor are also appreciated. The support from the Australian Research Council Discovery Project (ARC-DP) and ARC Industry Transformation Training Centre for Advanced Technologies in Rail Track Infrastructure (ITTC-Rail) is gratefully appreciated.

References

ASTM. American Society for Testing and Materials (2011). "Standard method for consolidated drained triaxial compression test for soils." *D7181*, West Conshohocken, PA.

Been, K., and Jefferies, M.J. (1985). "A state parameter for sands". *Géotechnique,* 35(2), 99-112.

320 Carrera, A., Coop, M., and Lancellotta, R. (2011). "Influence of grading on the mechanical
321 behavior of Stava tailings". *Géotechnique*, 61(11), 935-946.

322 Chavez, C., and Alonso, E.E. (2003). "A constitutive model for crushed granular aggregates
323 which includes suction effects". *Soil and Foundations*, 43(4), 215-227.

324 Chiaro, G., Indraratna, B., Tasalloti, S.M.A., and Rujikiatkamjorn, C. (2013), "Optimisation
325 of coal wash-slag blend as a structural fill". *Ground Improvement,* 168(GI1), 33-44.

326 Fu, R., Coop, M.R., and Li, X.Q. (2017). "Influence of particle type on the mechanics of
327 sand-rubber mixtures". *J. Geotech. Geoenviron. Eng.*, 143(9), 04017059.

328 Indraratna, B., Sun, Q., and Nimbalkar, S. (2014). "Observed and predicted behavior of rail
329 ballast under monotonic loading capturing particle breakage". *Can. Geotech. J.*, 51, 1-14.

330 Indraratna, B., Qi, Y., and Heitor, A. (2017). "Evaluating the Properties of Mixtures of Steel
331 Furnace Slag, Coal Wash, and Rubber Crumbs Used as Subballast". *J. Mater. Civ. Eng.*,
332 30(1), 04017251.

333 Li, X.S., and Dafalias, Y.F. (2000). "Dilatancy for cohesionless soils". *Géotechnique*, 50(4),
334 449-460.

335 Mashiri, M., Vinod, J.S., Sheikh, M.N., and Tsang, H.H. (2015). "Shear strength and
336 dilatancy behavior of sand–tire chip mixtures". *Soil and Foundations*, 55(3), 517-528.

337 Mashiri, M., Vinod, J.S., Sheikh, M.N., and Carraro, J.A.H. (2017). "Shear modulus of sand–
338 tire chip mixtures". *Environmental Geotechnics*, 16.00016.

339 Modoni, G., Koseki, J., and Anh Dan, L.Q. (2011). "Cyclic stress-strain response of
340 compacted gravel". *Géotechnique*, 61(6), 473-485.

341 Nova, R., and Wood, D.M. (1979). “A constitutive model for sand in triaxial compression”.
342 *Intl J. Num. Anal. Methods Geomech.*, 3, 255-278.

343 Rowe, P.W. (1962). “The stress-dilatancy relation for static equilibrium of an assembly of
344 particles in contact”. *Proc. R. Soc.*, Ser. A 269, 500-527.

345 Salvatore, I., Giuseppe, M., Gabriele, C., and Erminio, S. (2015). “Predictive correlations for
346 the compaction of clean sands”. *Transportation Geotechnics*, 4, 38-49.

347 Sheikh, M.N., Mashiri, M., Vinod, J., and Tsang, H. (2013). “Shear and Compressibility
348 Behavior of Sand-Tire Crumb Mixtures”. *J. Mater. Civ. Eng.*, 25, 1366-1374.

349 Tasalloti, S.M.A., Indraratna, B., Rujikiatkamjorn, C., Heitor, A., and Chiaro, G. (2015). “A
350 laboratory study on the shear behavior of mixtures of coal wash and steel furnace flag as
351 potential structural fill”. *ASTM Geotechnical testing journal,* 38(4), 361-372.

352 Taylor, D.W. (1948). *Fundamental of soil mechanics,* New York, Wiley.

353 Wan, R.G., and Guo, P.J. (1998). “A simple constitutive model for granular soils: modified
354 stress-dilatancy approach”. *Computers and Geotechnics*, 22(2), 109-133.

355 Wang, Z.L., Dafalias, Y.F., and Shen, C.K. (1990), “Bonunding surface hypoplasticity model
356 for sand”. *J. Engng Mech.*, 116 (5), 983-1001.

357 Wood, D.M., and Belkheir, K. (1994). “Strain softening and state parameter for sand
358 modelling”. *Géotechnique*, 44(2), 335-339.

359 Youwai, S., and Bergado, D.T. (2003). “Strength and deformation characteristics of shredded
360 rubber tire-sand mixtures”. *Canadian Geotechnical Journal*, 40(2), 254-264.

361 Zheng, Y.F., and Sutter, G.K. (2000). “Dynamic properties of granulated rubber/sand
362 mixutres”. *Geotechnical Testing Journal*, 23(3), 338-344.

363 Zornberg, J.G., Viratjandr, C., and Cabral, A.R. (2004). “Behavior of tire shred–sand
364 mixtures”. *Canadian Geotechnical Journal*, 41(2), 227–241.

Figures list

384 **Table list**

Table 1 Critical state and total work parameters for SFS+CW+RC mixtures

	Mixtures	RC (%)	Test No.	σ'_3(kPa)	Dry density (kN/m^3)	M_{cs}	e_0	e_{cs}	W_{total} (kPa)	Γ	λ
Group A	SFS70+CW30	0	CD-1	10	19.290	1.94	0.292	0.395	2.18	0.606	0.062
			CD-2	40	19.285	1.804	0.263	0.328	9.02		
			CD-3	70	19.298	1.739	0.231	0.281	10.79		
	SFS63+CW27+RC10	10	CD-4	10	16.695	2.01	0.271	0.395	4.84	0.740	0.101
			CD-5	40	16.722	1.613	0.234	0.292	14.80		
			CD-6	70	16.708	1.548	0.203	0.235	31.18		
	SFS49+CW21+RC30	30	CD-7	10	14.735	2.0	0.271	0.401	5.46	0.94	0.159
			CD-8	40	14.742	1.61	0.220	0.236	21.93		
			CD-9	70	14.725	1.48	0.200	0.162	38.58		
Group B	SFS56+CW24+RC20	20	CD-10	10	13.139	1.98	0.246	0.416	5.95	0.890	0.141
			CD-11	40	13.145	1.55	0.212	0.263	18.66		
			CD-12	70	13.148	1.51	0.171	0.198	33.82		
	SFS42+CW18+RC40	40	CD-13	10	11.789	1.8	0.250	0.390	5.81	1.012	0.183
			CD-14	40	11.785	1.5	0.208	0.216	23.28		
			CD-15	70	11.793	1.43	0.164	0.148	42.74		

*The mixtures are expressed as SFS+CW+RC, and the numbers after SFS, CW, and RC are the percentages of steel furnace slag, coal wash, and rubber crumbs by weight. CD refers to consolidated drained triaxial tests, and e_0 is the initial void ratio after consolidation. Test data from Group A were used to calibrate Equations (5, 6, and 8), and Group B was used for validation.

391 Table 2 Model parameters for SFS+CW+RC mixtures

	Mixtures	RC (%)	σ'_3(kPa)	m	d_0	
Group A	SFS70+CW30	0	70	-1.30	3.03	Γ_1 =0.064 $\Gamma_2 = 0.01$ $\lambda_1 = 0.069$ $\lambda_2 = 0.003$ $\alpha = -0.117$ $M_0 = 2.258$
	SFS63+CW27+RC10	10	10	-0.46	2.95	
			40	-2.15	2.17	
			70	-2.86	1.83	
	SFS49+CW21+RC30	30	10	-0.93	3.80	
			40	-2.36	3.29	
			70	-4.16	2.49	
Group B	SFS56+CW24+RC20	20	10	-0.53	5.12	M^*_{cs} =1.83
			40	-2.98	2.18	M^*_{cs} =1.60
			70	-5.29	3.19	$M^*_{cs} = 1.50$
	SFS42+CW18+RC40	40	10	-0.76	3.27	$M^*_{cs} = 1.84$
			40	-2.48	2.45	$M^*_{cs} = 1.53$
			70	-4.01	3.05	$M^*_{cs} = 1.46$

392 *Group A was based on the test data, and Group B was based on the Equations (8 and 10).

393

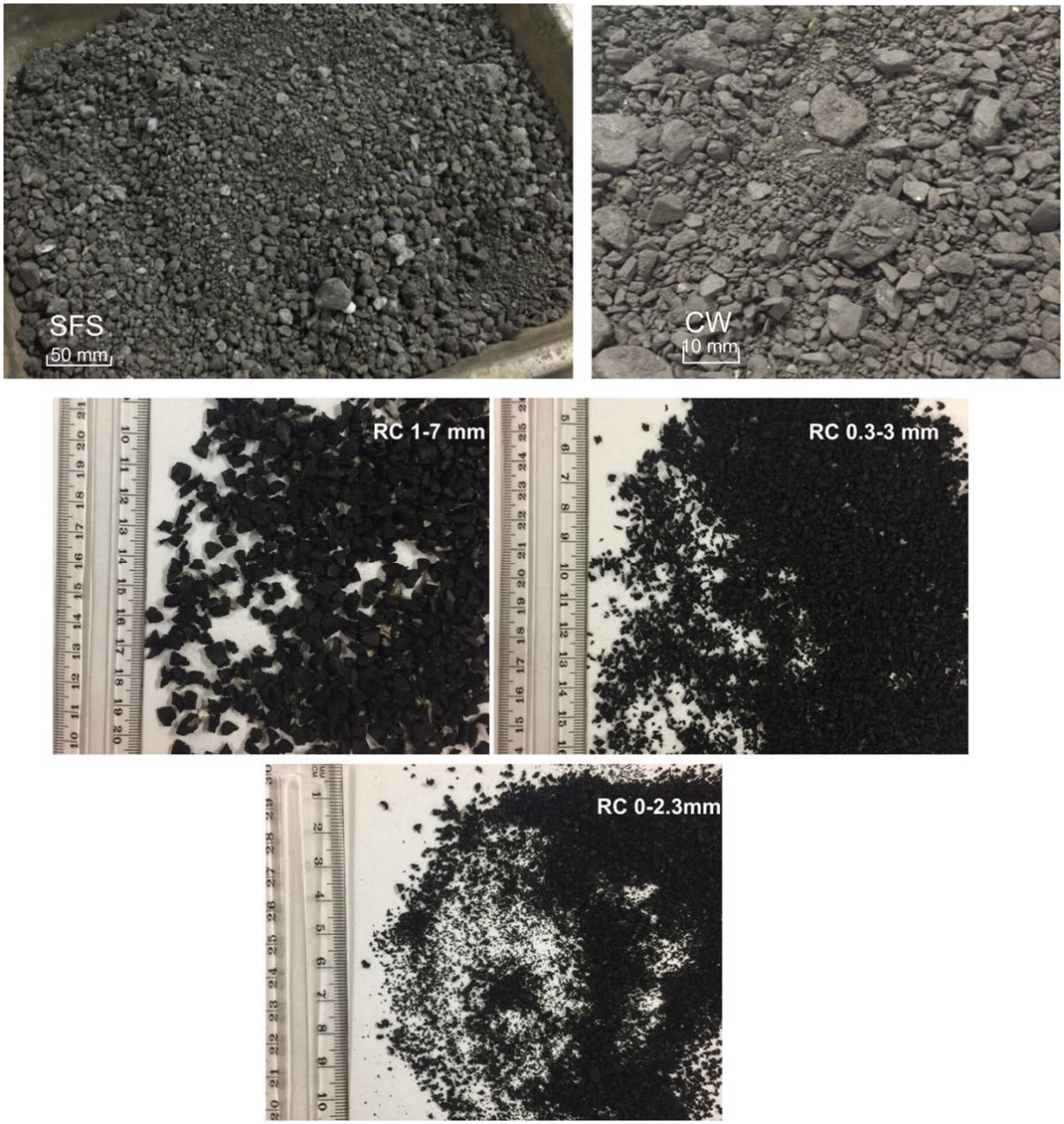

394

395 Fig.1 The waste materials used in this study

396

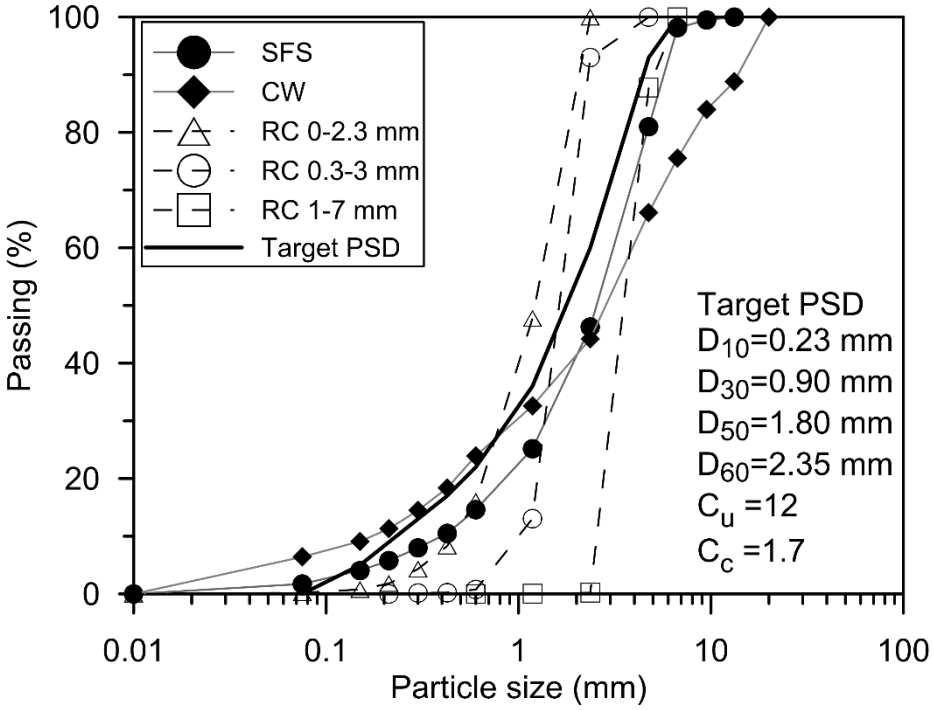

397

398 Fig.2 Particle size distribution of the waste materials and the target PSD

399

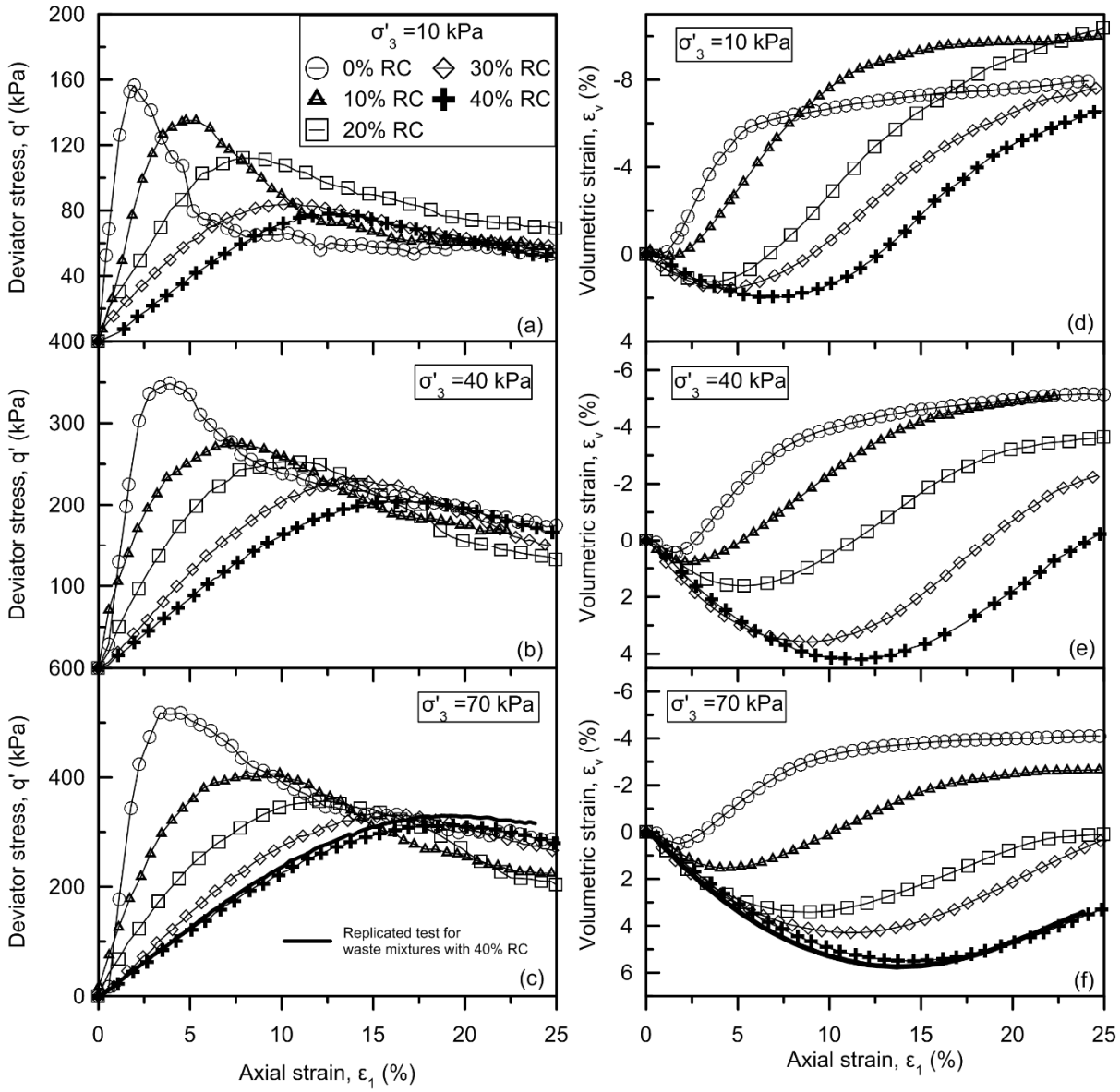

400

401 Fig.3 Stress-strain curves for the SFS+CW+RC mixtures with different R_b (%): (a)-(c)

402 deviator stress versus axial strain; (d)-(f) volumetric strain versus axial strain

403

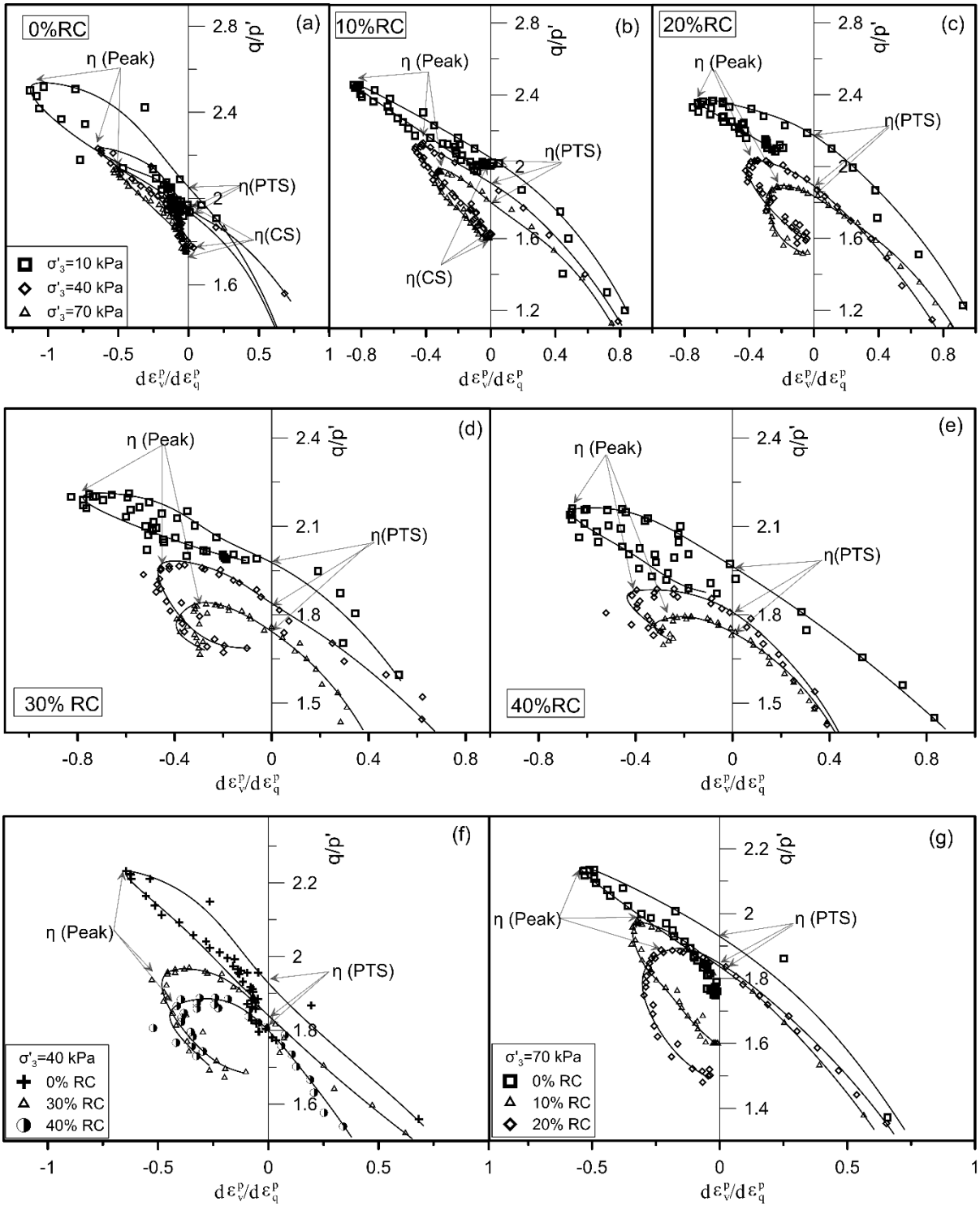

404

405 Fig.4 Stress ratio-dilatancy curve of SFS+CW+RC mixtures (a) with 0% RC, (b) with 10%

406 RC, (c) with 20% RC, (d) with 30% RC, (e) with 40% RC, (f) at $\sigma'_3 = 40\ kPa$, (g) at $\sigma'_3 =$

407 $70\ kPa$

408

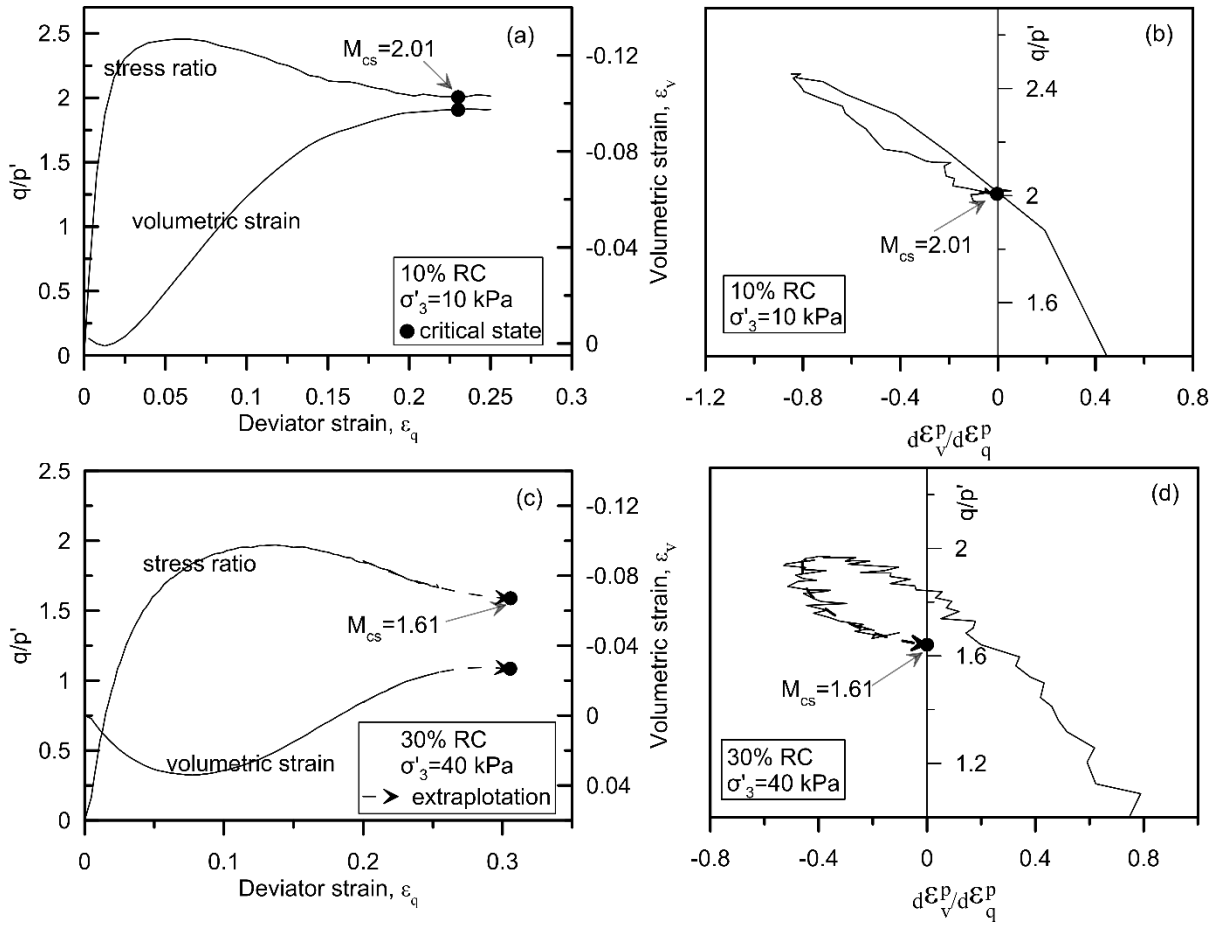

409

410 Fig.5 Determination of the critical point for waste mixtures: (a) the stress-strain curve, and (b)

411 the stress ratio-dilatancy curve for 10% RC at $\sigma'_3 = 10\ kPa$; (c) the stress-strain curve, and

412 (d) the stress ratio-dilatancy curve for 30% RC at $\sigma'_3 = 40\ kPa$

413

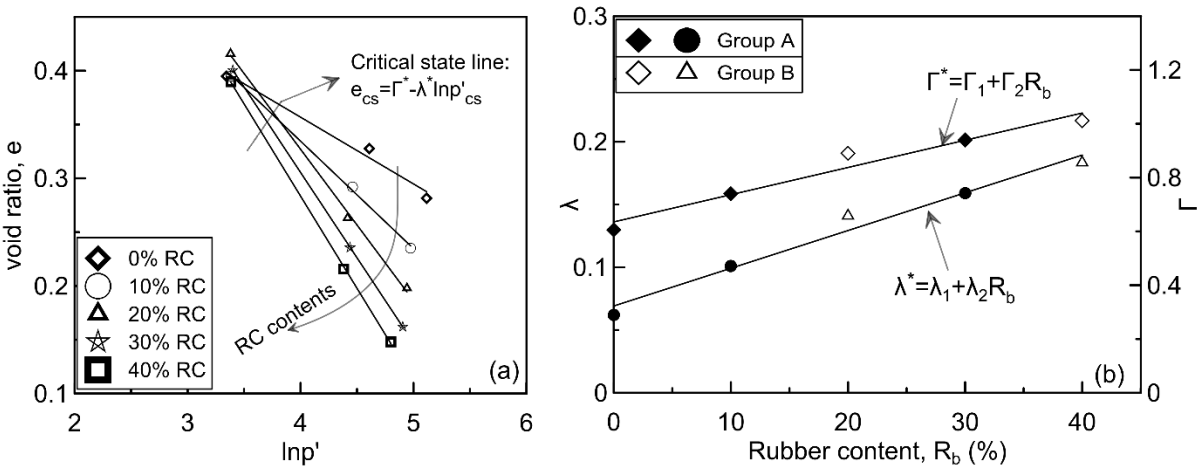

414

415 Fig.6 (a) $e - \ln p'$ curves for waste mixtures at critical state; (b) the relationship of Γ and λ in

416 terms of $R_b(\%)$

417

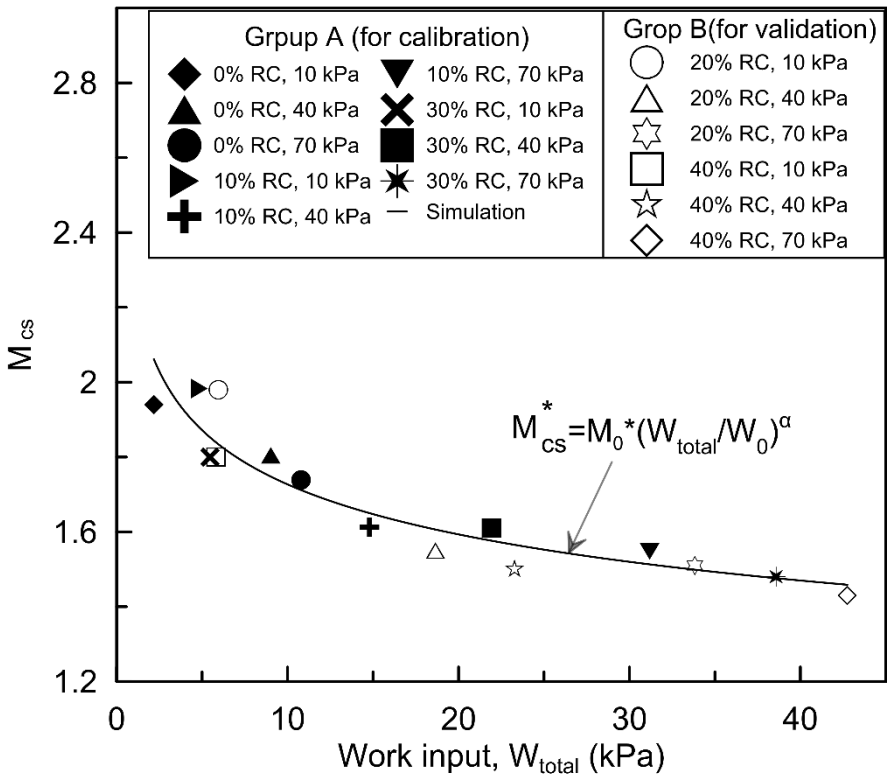

418

419 Fig.7 The relationship of W_{total} and critical stress ratio M_{cs} for SFS+CW+RC mixtures

420

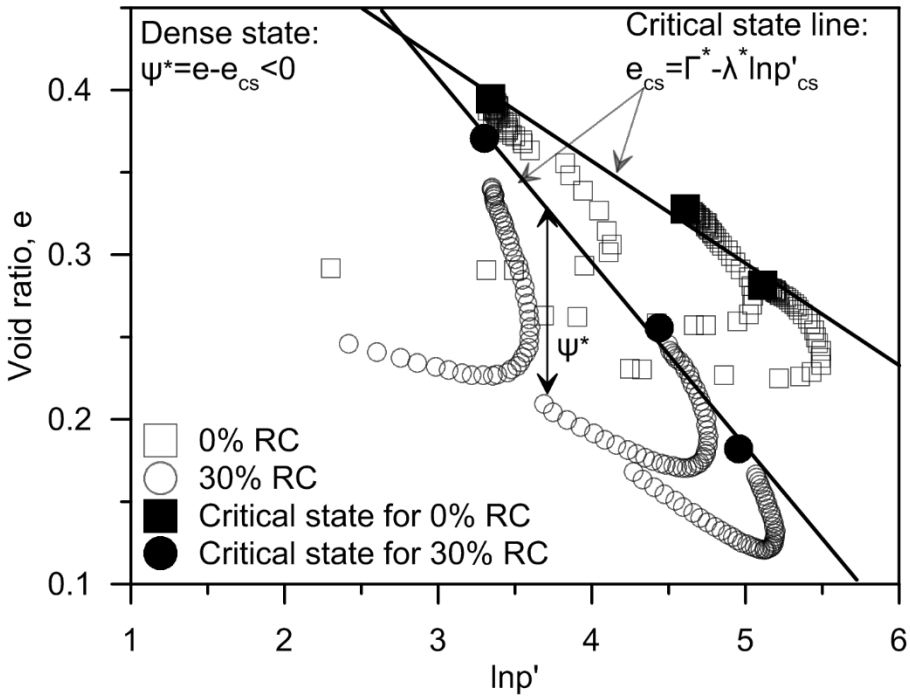

421

422 Fig.8 Definition of the state parameter and the critical state line for the SFS+CW+RC mixture

423 (SFS:CW=7:3) having 0% and 30% RC

424

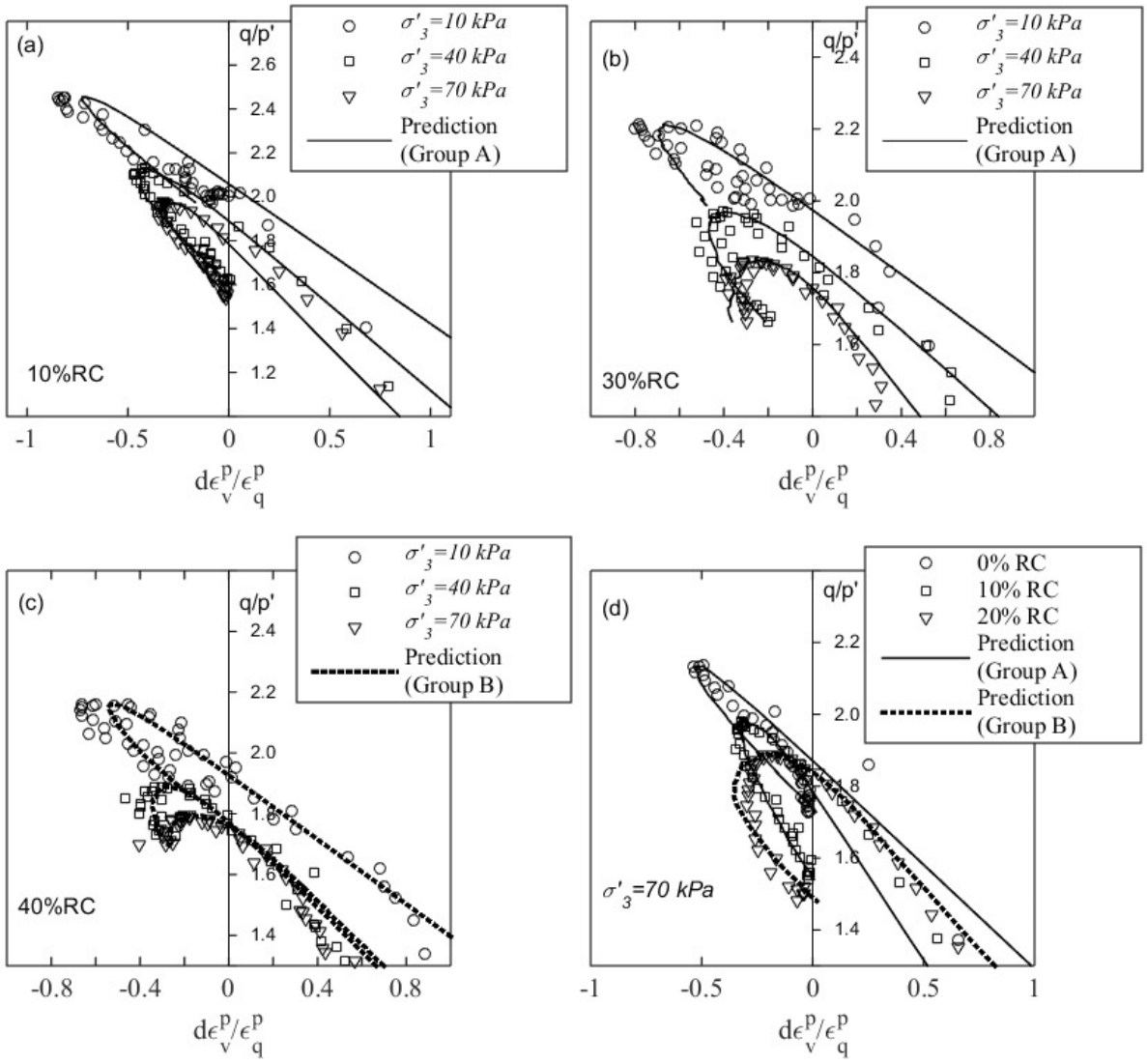

425

426 Fig.9 Comparison of tests results and model predictions (stress ratio versus dilatancy) for

427 waste mixtures (SFS:CW=7:3) (a) with 10% RC, (b) with 30% RC, (c) with 40% RC, (d)

428 with different R_b at $\sigma'_3 = 70\ kPa$